INTERNATIONAL JOURNAL OF HYDROGEN ENERGY XXX (2017) 1–12

Available online at www.sciencedirect.com

ScienceDirect

journal homepage: www.elsevier.com/locate/he

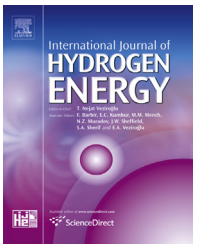

Reliability assessment of a stand-alone wind-hydrogen energy conversion system based on thermal analysis

Omid Alavi[*], *Abbas Hooshmand Viki*, *Mohammad Tavakoli Bina*, *Mohsen Akbari*

Department of Electrical Engineering, K.N. Toosi University of Technology, Tehran, Iran

ARTICLE INFO

Article history:
Received 23 January 2017
Received in revised form
16 March 2017
Accepted 1 April 2017
Available online xxx

Keywords:
Reliability assessment
Wind-hydrogen hybrid system
Thermal analysis
MIL-HDBK-217
Buck converter

ABSTRACT

Due to the stochastic behavior of the wind speed, accessing the wind energy would be problematic in some critical moments. One feasible solution lies in the use of wind turbines to produce hydrogen through an electrolyzer and by using wind-hydrogen hybrid systems. However, many of the issues related to these systems should be investigated to make landmark decisions about their performance. For instance, there is a lack of study on the reliability assessment of the wind-hydrogen systems; for this purpose, the main objective of this study is to evaluate the reliability of a stand-alone wind-hydrogen energy conversion system unconnected to the grid. The proposed system consists of two major parts: the rectifier and the buck converter. The primary task of the rectifier is to rectify the wind turbine output voltage to a constant DC voltage. Additionally, the buck converter is responsible to reduce the voltage level to a 48 V voltage, which meets the voltage requirement of the 3.6 kW electrolyzer. The results of the performed simulations showed that the rectifier is under more thermal stresses than the buck converter. The predicted mean time to failure (MTTF) of the hybrid system is approximately 7.6 years, and this estimation can affect the maintenance and refurbishment costs.

Introduction

Wind is the most favorable renewable forms of energy among different renewable resources. However, the uncertainty of wind speeds causes several problems in long-term planning and other aspects of wind project. Additionally, this issue will limit the availability of energy, especially in stand-alone networks. Consequently, storing energy generated by the wind turbine as a gas or liquid can be a solution to address this issue.

Hydrogen has various advantages compared to the other flammable gases. It can be extracted using different methods, such as water electrolysis, fossil fuels, photovoltaic, and chemical reactions [1]. The use of hybrid energy systems can be improved the overall performance so that each component can overcome the weaknesses related to the other parts [2]. Nevertheless, the utilization of wind turbines in order to produce and store hydrogen can highlight strengths of each system.

There are many researches on the hydrogen production from wind energy. Siyal et al. [3] performed an economic analysis of a stand-alone wind-to-hydrogen system to refuel vehicles and help road transportation. The evaluations of

* *Corresponding author.*
E-mail address: alavi.omid@mail.com (O. Alavi).

http://dx.doi.org/10.1016/j.ijhydene.2017.04.006

three stations in Sweden were made by using the HOMER software. They concluded that the used energy conversion system will offer both economic and environmental benefits, particularly in a large scale. Ref. [4] optimized the design and operation of the complete wind-hydrogen-electricity networks using the general mixed integer linear programming energy network model. The optimal wind turbine locations were identified using the geographic information system (GIS) by considering ten different environmental and technical constraints. The obtained results confirmed that the utilization of a well-designed wind-hydrogen energy conversion system can satisfy the overall energy for Britain's domestic transport.

Mostafaeipour et al. [5] evaluated the suitability of wind energy for hydrogen production in the province of Fars, Iran. Four different large-scale wind turbines installed in the windiest station were analyzed to assess the ability of the proposed wind/hydrogen system in fueling cars. The outcomes showed that a 900 kW wind turbine will be sufficient for fueling approximately 22 cars per week.

Olateju et al. [6] made a technical and economic assessment for producing hydrogen from a large-scale wind turbine installed in Western Canada. The size and number of the electrolyzer units and also energy storage capacity were optimized by minimization of the hydrogen production cost based on the real-time wind data. After running the simulations, they found that the minimum cost for a case study will occur when the electrolyzer and battery capacity factors are roughly equal. However, they concluded that the cost of hydrogen production from wind energy would be prohibitive compared to the fossil fuel-based systems.

Hacatoglu et al. [7] assessed the sustainability of a wind-hydrogen system to supply the energy of a small-scale station – including 50 households – in Ontario, Canada. They used a new index for evaluating the best possible system based on six category indicators and 20 sub-indicators. Additionally, the performance of the wind-hydrogen energy system was compared to a gas-fired system. The results demonstrated that the novel index shows a very little difference between the two systems. Nevertheless, they suggested that multi-criteria and comprehensive analyses are necessary to investigate the sustainability.

Ref. [8] studied the environmental impacts related to wind/hydrogen hybrid systems. By considering all greenhouse gas (GHG) emissions from wind energy harvesting to hydrogen production, a life cycle assessment was carried out to specify the emissions per amount of hydrogen production. In addition, the influence of the variations of several input parameters on the GHG emissions was shown by performing an uncertainty analysis. The results indicated that a wind/hydrogen system can reduce approximately 94% of the emissions in comparison with a conventional fossil fuel-based system. Generally, the utilizing of a wind-to-hydrogen energy system can lead to a remarkable reduction in GHG emissions.

Using the non-grid-connected wind/hydrogen energy conversion systems can decrease the number of auxiliary equipment for providing stable grid connection, increase the rated wind power, and contribute to the further development of massive wind farms. With these advantages, the use of this type of energy conversion system will increase efficiency and reduce costs. In Ref. [9], the wind turbine without the presence of the grid supplied the water electrolyzer directly. They made some changes in order to improve the overall technical performance. The adopted approach in that paper has been used to create a balance between the current and voltage so that the total current remains constant as well as the total capacity of all wind turbines is used. The obtained results showed that the variations of current density can only affect the gas output, and its influence on the current efficiency and gas quality is negligible.

Chade et al. [10] investigated an integrated wind/hydrogen system in order to support the infrastructure of fuel fossils for a small Icelandic island. HOMER software was used to simulate energy balance and also determine the optimal size of the system's components. The outcomes from this analysis illustrated that the examined infrastructure can be a practical solution with a payback period of four years.

Aiche-Hamane et al. [11] evaluated the suitability of hydrogen production from a Bergey Excel 10 kW wind turbine installed in the station at Ghardaia, Algeria. The results of this study revealed that the hub height of wind turbines can have a dramatic impact on the capability of hydrogen production.

In Ref. [12], a study on wind-hydrogen energy conversion systems was conducted. The performed analysis included economic computations, hydrogen cost estimates, and sizing the components. Additionally, two different systems – a grid-connected system and an isolated system – situated in a Norwegian island were selected as case studies. The grid-connected system offered more economic benefits; however, it requires frequent grid interaction.

By expanding the use of renewable energy sources, the role of power electronic devices has become more important. Today, power electronic converters are extensively used in various household and industrial applications. One of the most common power electronic converters is the family of DC–DC converters, which is utilized frequently in photovoltaic and wind energy conversion systems. In the past six decades, DC–DC converters have undergone tremendous changes and thus the result of this attention was 500 types of these converters. There are several topologies for DC–DC converters; however, they can be divided into three fundamental categories based on the input and output voltage levels: buck, boost, and buck-boost converters. What is important here is to provide a suitable performance including high output quality, longer lifetime and lower energy losses. These factors can be explained by the concept of reliability.

The reliability of a power electronic converter as a commercial product is important from an economic standpoint, because higher reliability means increased useful life and therefore exhibits better competition in the market. There are various studies on the reliability related to the hydrogen applications. In Ref. [13], a complete review of failure modes and performance degradation for hydrogen-based polymer electrolyte fuel cells (PEFCs) was conducted. It identifies 22 different frequent faults by considering all failure-prone components. Also, the processes leading to performance degradation are classified in terms of activation, mass

Please cite this article in press as: Alavi O, et al., Reliability assessment of a stand-alone wind-hydrogen energy conversion system based on thermal analysis, International Journal of Hydrogen Energy (2017), http://dx.doi.org/10.1016/j.ijhydene.2017.04.006

transportation, ohmic, and efficiency losses. By continuing this study, Whiteley et al. [14] made a reliability analysis of PEFCs using the Petri-Net analysis and fuel cell modelling techniques. Their work improved the previous methods for estimating fuel cell reliability by adding operating parameters, drive cycles, and dependencies between multiple failure modes. Several studies also evaluated the reliability of hydrogen sensing devices (e.g., hydrogen safety sensors) under different environmental conditions [15–17]. Among a wide range of researches on the reliability of applications related to hydrogen, there is certainly a lack of detailed study on estimating reliability and lifetime of power electronic devices used in hydrogen energy conversion systems. In recent years, several examinations on the reliability of power electronic devices are also carried out. To the best of our knowledge, it is the first time that the reliability of wind-hydrogen conversion systems is assessed based on an accurate thermal model by considering feedback from the case temperature.

The objective of this study is to evaluate the reliability of a stand-alone wind-hydrogen energy conversion system based on the thermal analysis. As the power electronic devices are known as the most failure-prone components in the energy conversion systems, the main focus of this paper is to perform simulations on these parts. In this paper, a 3.6 kW water electrolyzer was used in the performed analysis, and it needs to be supplied by a 48 V voltage. The proposed system consists of a three-phase rectifier and a buck DC–DC converter. The rectifier side is responsible to rectify the wind turbine output voltage to a regulated DC voltage. Then, the buck converter will reduce the voltage level to 48 V. According to the direct relationship between the reliability and the operating temperature of the semiconductor devices (switch and diode), the analysis will continue by determining the temperatures using a thermal network modeling, and showing their thermal behavior.

The rest of the paper is organized as follows. Section The proposed wind-hydrogen hybrid system gives a brief description of the proposed wind-hydrogen energy conversion system. The principles of reliability and the employed standard are explained in Section Methodology. The equations related to the different components' failure rate are also addressed in this section. The methodology based on the lookup table method and thermal analyses is discussed in the second part of Section Methodology. The results and discussion are presented in Section Results and discussion. Finally, the conclusions are given in Section Conclusion.

The proposed wind-hydrogen hybrid system

Regarding the issues related to the uncertainty of wind turbines due to the probabilistic behavior of the wind, converting wind energy into hydrogen and storing it in a repository will enhance the reliability and availability. There are different topologies for hybrid wind-hydrogen systems. The Hydrogen Research Institute (HRI) presented a stand-alone energy system for hydrogen production by wind and solar energies. When the input energies are more than the required AC load, the additional energy will be converted into the hydrogen using an electrolyzer. Typically, all renewable components are connected together on a 48 V DC bus [18]. In this study, a wind-hydrogen energy conversion system shown in Fig. 1 is proposed. This system serves as a stand-alone generation, and does not have any connection to the grid.

It is evident from Fig. 1 that the output voltage of wind turbine is AC that can supply any type of AC load. This is despite the fact that the required voltage for producing hydrogen by electrolysis should be direct current (DC). The electrolyzer voltage must be fixed at 48 V DC. However, the current through the electrolyzer should be sufficiently enough to enhance the process of hydrogen production from water. For this reason, the output power of the buck converter is in range of kilowatts to generate a high output current at a low output voltage. In the first stage, the AC voltage will be rectified by using a three-phase AC-DC rectifier consisting of six insulated-gate bipolar transistors (IGBTs) and six diodes. Then, the buck converter reduces the generated DC voltage to a fixed value of 48 V. The buck converter is composed of an IGBT, a diode, and an LC filter. A sinusoidal pulse-width modulation (SPWM) is responsible for producing switching states of the rectifier side. Additionally, an open-loop scheme is selected for the buck converter. The switching frequency is considered to be equal to 5 kHz for both sides.

Hahn et al. [19] conducted a comprehensive study on the causes of failure in the wind turbine's systems. This study set out to examine the downtimes caused by the malfunctions and damaged components based on the extracted data from 1500 operating wind turbines over a 15 years period. The summary of this study was to emphasize the importance of reliability of power electronic devices as primary source of failure in wind turbine energy conversion systems. In addition, another similar study confirmed that blades, control system and electric system are common causes of failure in wind systems [20]. Nevertheless, ignoring the other

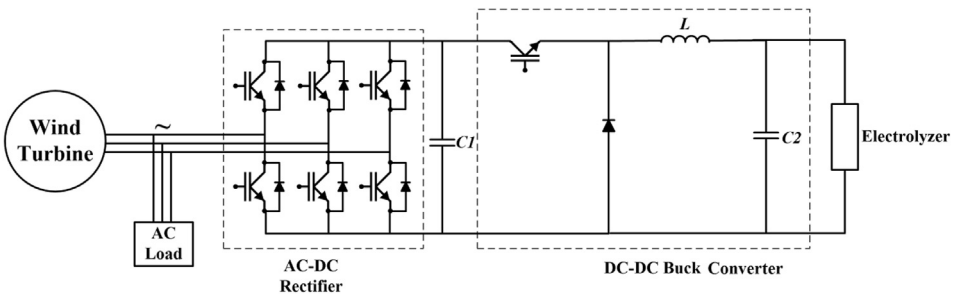

Fig. 1 – The proposed wind-hydrogen hybrid system.

Please cite this article in press as: Alavi O, et al., Reliability assessment of a stand-alone wind-hydrogen energy conversion system based on thermal analysis, International Journal of Hydrogen Energy (2017), http://dx.doi.org/10.1016/j.ijhydene.2017.04.006

mechanical failures and considering the output of the wind turbine as a three-phase voltage source will be permitted. In this paper, the output voltage of the wind turbine is 400 V AC [21], and the output power of the buck converter is considered 3.6 kW. Hence, the electrolyzer current should be 75 A when its voltage is 48 V. The output voltage level of the buck converter has a direct relationship with its output voltage level [22], and the conversion ratio is M(D) = D. Where D represents the duty cycle which demonstrates the ratio of on-time to the cycle time.

The DC output voltage of the rectifier is almost 692 V, because the line-to-line voltage will be appeared in the rectifier output. Thus, the value of the duty cycle must be 6.93%.

Methodology

Reliability assessment

To predict the failure rate of electronic components, there are two widely used procedures, namely MIL-HDBK-217 [23] and FIDES [24]. The MIL-HDBK-217 is the first reliability standard and updated in 1995, while the FIDES was updated for the last time in 2009. Nevertheless, the second standard due to the high complexity and different information in various working conditions of the electronic components has not been welcomed. Therefore, the MIL-HDBK-217 is utilized in this paper. In this standard, for the elements used in power electronic circuits, numerous relationships and conditions have been considered to determine the failure rate, which thermal analysis must be performed accurately for semiconductors.

One of the essential issues that requires attention and conscious awareness is heat dissipation and heat transfer through the power electronic device. During operation, the components used in a power converter will never attain 100% efficiency with regard to the switching and conduction losses. The conduction losses occur when the component is turned on and the current is passing through it. Additionally, the switching losses represent power losses during the transition between the switching-on and switching off. For instance, approximately 2–10% of the power of an IGBT motor driver is wasted as the heat dissipation [25].

Heat generated due to the power losses should be transferred from the equipment to the environment by a heatsink. The selection of improper cooling system can affect on the electronic equipment's performance, the device capability, and also the reliability.

More efficient use of any device, has always been a goal of manufacturers. In power electronics, this purpose will be fulfilled with the utilization of several cases, such as high-quality output, longer life, and lower energy consumption. In fact, a converter with higher lifespan is more reliable, and reliability also shows the possibility of system failure at the specified time. Reliability of a system depends on various factors; therefore, the system should be divided into smaller parts to assess its reliability, and then the reliability of each component should be estimated [26]. Generally, four different indicators of failure rate, mean time to failure (MTTF), mean time to repair (MTTR), and availability were considered to determine the reliability [27]. Thus, the basic concepts should be defined.

Reliability is defined as the ability of an item to perform a desired function under the stated conditions at a particular time interval. The reliability is frequently measured as the probability or frequency of failure [28]. Failure occurs when the system cannot operate for any reason. Therefore, the operation time without system downtime is generally a random variable that can sometimes be long or short. In addition, failures can be divided into two categories: cataleptic and degradation [29]. The failure rate plays a prominent role in evaluating the reliability of a system. Considering the symbol of λ as the failure rate and the exponential distribution for failures, the reliability function will be as follows [30]:

$$R(t,\lambda) = e^{-\lambda t} \tag{1}$$

The value of the failure rate will result in a suitable analysis of reliability, and it is enough for the further evaluations.

MTTF expresses the average time between starting time and the first of its failure. This failure is such that the device is not able to continue their expected functions. MTTF is usually estimated in an hour or thousand hours. The relationship between the MTTF and the reliability function is as follows:

$$MTTF = \int_0^{+\infty} R(t)dt \tag{2}$$

By substituting Eq. (1) in Eq. (2), the MTTF will be equal to the inverse of the failure rate [31].

$$MTTF = 1/\lambda \tag{3}$$

In recent decades, several procedures for estimating reliability have been introduced by different organizations. The first reliability procedure (TR-1100) was published by the United States and under the Rome Air Development Center (RADC) in 1956. The standard provides the failure rate models for computer and electronic components [32]. After the publication of this standard, MIL-HDBK-217 as a reliability guidebook was released and become the most popular standard among various procedures.

The MIL-HDBK-217 provides the failure rates of all electronic components. The standard introduces two methods for assessing the reliability: parts count and parts stress. The results from the parts count method will lead to a higher failure rate or lower reliability. In other words, the parts count method is more conservative than the parts stress approach. The parts stress method when the design phase is completed and components' stress are available, is applicable [26].

The related formulas of the failure rates consist of the base failure rate for each component. The failure rates will change by applying π_i factors, which show the operation conditions. Thus, the exact determination of these factors would make the analysis more accurate, especially in the semiconductors.

With respect to the standard's approach, the following equation can be employed to identify the total failure rate of a system [33]:

$$\lambda_{Total} = \sum_{i=1}^{n} N_i \lambda_i \tag{4}$$

Please cite this article in press as: Alavi O, et al., Reliability assessment of a stand-alone wind-hydrogen energy conversion system based on thermal analysis, International Journal of Hydrogen Energy (2017), http://dx.doi.org/10.1016/j.ijhydene.2017.04.006

where n is the number of independent elements, N_i presents the number of the similar elements. λ_i and λ_{Total} are respectively the components' failure rate and the total failure rate.

IGBT failure rate

Nowadays, using the metal–oxide–semiconductor field-effect transistors (MOSFETs) and IGBTs as the switch in power electronic devices is preferred. Both of these types of switch are power semiconductors used in high efficiency and fast switching circuits. Although the structure of the MOSFET and IGBT looks very similar, their substrates are different and this difference has led to enormous impact on their performance. MOSFETs are preferred in output powers less than 500 W, while IGBTs are typically utilized in low-frequency and high output power applications. Another feature that provides IGBT more proper than the MOSFET is its ability to operate at high junction temperatures (more than 100 °C). Considering the circuit used in the study, the IGBT will be employed [34].

IGBT is not directly mentioned in the MIL-HDBK-217 standard; thus, the popular approach of using MOSFET relations for IGBT has been used for finding π-factors [35]. The IGBT relationships have been proposed as low-frequency Si FET transistors in Chapter 6 of the used standard.

The failure rate of IGBT is as follows:

$$\lambda_p = \lambda_b \pi_T \pi_A \pi_Q \pi_E \tag{5}$$

where π_T, π_A, π_Q, π_E, λ_b, and λ_p are the temperature factor, the application factor, the quality factor, the environment factor, the base failure rate (failures/10^6 h) and the predicted failure rate of IGBT, respectively.

According to the standard, the base failure rate of IGBT is considered 0.012 *failures*/10^6 h. The temperature factor is one of the most influential factors in determining the reliability of semiconductors. Therefore, appropriate estimation of this factor, which is dependent on the junction temperature according to the following equation, seems crucial.

$$\pi_T = \exp\left(-1925\left(\frac{1}{T_j+273}-\frac{1}{298}\right)\right) \tag{6}$$

where T_j is the junction temperature.

Quality and environment factors also have great impact on calculating the reliability, and their values can be considered 5.5 and 1.0, respectively.

Additionally, the application factor is only related to the power output level, and its value is equal to 10 for the rated output powers above 250 W. Thus, the failure rate of IGBT can be mentioned as follows:

$$\lambda_p = 0.66 \times \exp\left(-1925\left(\frac{1}{T_j+273}-\frac{1}{298}\right)\right) \tag{7}$$

where T_j is the steady state junction temperature.

Diode failure rate

The failure rate of diode is as follows:

$$\lambda_p = \lambda_b \pi_T \pi_S \pi_C \pi_Q \pi_E \tag{8}$$

where π_S and π_C are electrical stress and contact construction factors, respectively.

Generally, diodes are utilized as power rectifiers in power electronic circuits. In industry, the diode with reverse recovery rate of less than 500 ns is chosen as fast. For times less than 100 ns, the diode would be ultra-fast [36]. Hence, the base failure rate of diode, in accordance to the MIL-HDBK-217 standard, is 0.025.

To estimate the temperature factor of the diode, the following equation can be used:

$$\pi_T = exp\left(-3091\left(\frac{1}{T_j+273}-\frac{1}{298}\right)\right) \tag{9}$$

where T_j is the junction temperature in terms of Celsius degree.

Another factor for the diode is electrical stress factor, which applies the voltage level in the failure rate. If the voltage stress is defined as the ratio of the applied voltage to the rated voltage, we will have:

$$V_S = \frac{Voltage\ Applied}{Voltage\ Rated} \tag{10}$$

According to the standard, the electrical stress factor of diode can be obtained as follows:

$$\pi_S = \begin{cases} 0.054 & (V_S \le 0.3) \\ (V_S)^{2.43} & (0.3 < V_S \le 1) \end{cases} \tag{11}$$

where V_S is the voltage stress.

The values of π_C, π_Q, and π_E are 1.0, 5.5 and 1.0 for the diode, respectively. Thus, the equivalent formula for the diode failure rate is as follows:

$$\lambda_p = 0.1375 \times \pi_S \times exp\left(-3091\left(\frac{1}{T_j+273}-\frac{1}{298}\right)\right) \tag{12}$$

Capacitor failure rate

The failure rate of capacitor can be obtained from Eq. (13).

$$\lambda_p = \lambda_b \pi_{CV} \pi_Q \pi_E \tag{13}$$

where π_{CV} exhibits the capacitance factor.

The base failure rate of the capacitor can be expressed as follows:

$$\lambda_b = 0.00086\left[\left(\frac{S}{0.4}\right)^5+1\right]\exp\left(2.5\left[\left(\frac{T_A+273}{273+T_R(max)}\right)^{18}\right]\right) \tag{14}$$

In Eq. (14), S is the ratio of the operated voltage to the rated voltage, T_A is the ambient temperature, and $T_R(max)$ is the maximum allowable temperature for capacitor (85 °C or 125 °C).

Additionally, the capacitance factor can be indicated by

$$\pi_{CV} = 1.2C^{0.095} \tag{15}$$

where C is the capacitance in microfarad.

The quality and environment factors for capacitor are 7.0 and 1.0, respectively. Nevertheless, the failure rate of the capacitor can be represented by Eq. (16).

$$\lambda_p = 8.4 \times \lambda_b \times (C_{\mu F})^{0.095} \tag{16}$$

Inductor failure rate

The formula of the inductor failure rate has an operation temperature which requires testing procedures and

Please cite this article in press as: Alavi O, et al., Reliability assessment of a stand-alone wind-hydrogen energy conversion system based on thermal analysis, International Journal of Hydrogen Energy (2017), http://dx.doi.org/10.1016/j.ijhydene.2017.04.006

complicated processes [26]. Therefore, the total failure rate of the inductor can be considered approximately 1.05×10^{-8} failures/hours.

MATLAB simulation

Typically, losses in the semiconductor components can be divided into three categories [37]:

- Conduction losses
- Switching losses
- Blocking losses

The blocking loss is very low and negligible. Nevertheless, the total losses of semiconductors are the sum of the conduction and switching losses. The approach used in this research is the practical outcomes presented in the datasheet of the intended IGBT module. In accurate models for estimating the power losses, any parameter will be temperature-sensitive parameter (TSP) which should be considered in the calculations. The IGBT conduction losses can be illustrated by a series connected DC voltage source (V_{CE0}) and a collector-emitter on-state resistance (r_C) [37]:

$$V_{CE}(i_C) = V_{CE0} + r_C i_C \tag{17}$$

This relationship demonstrates the dependency between the Collector-Emitter voltage and the Collector current. The IGBT conduction losses can be obtained by

$$P_{C_{IGBT}} = V_{CE}(i_C) \times i_C \tag{18}$$

The graphs provided in the datasheet represent the dependency of V_{CE} to the junction temperature. Therefore, the above relationship will change as follows:

$$P_{C_{IGBT}} = V_{CE}(i_C, T_j) \times i_C \tag{19}$$

By taking the effect of temperature, the diode conduction losses will be as follows:

$$P_{C_D} = V_F(i_F, T_j) \times i_F \tag{20}$$

The on-state energy losses in the IGBT can be determined as the total switch on-state energy regardless of the reverse recovery and on-state energy of freewheeling diode reverse recovery.

$$E_{on_{IGBT}} = E_{on_{Ti}} + E_{on_{Trr}} \tag{21}$$

The on-state diode energy is often included reverse recovery energy.

The IGBT turn-off energy losses are determined in the same manner. The turn-off losses in the diode are usually negligible. Thus, the IGBT and diode switching losses can be obtained by multiplying energies by the switching frequency.

According to the figures provided in the datasheet of the nominated module, the turn-on and turn-off energies of the IGBT and diode reverse recovery energy are presented in terms of the Collector current and different temperatures. The curves and values provided in the datasheet are specified for a particular supply voltage (V_{CC}). Therefore, these energies are related to the mentioned parameters as follows:

$$P_{S_{IGBT}} = \left(E_{on_{IGBT}}(i_C, T_j, V_{CC}) + E_{off_{IGBT}}(i_C, T_j, V_{CC})\right) f_{sw} \tag{22}$$

And for diode, we have:

$$P_{S_D} = E_{rec_D}(i_F, T_j, V_{CC}) f_{sw} \tag{23}$$

To determine the switching and conduction losses of diode and switch, the lookup table method is used so that 2D and 3D lookup tables must be utilized in the MATLAB environment. Detailed explanations of the procedure for identifying these power losses can be found in Ref. [38].

Usually, thermal conductivity is the dominant in comparison to the heat transfer process so that it is assumed that convection and thermal radiations are negligible [39]. There are two different approaches for modeling resistance-capacitance (RC) thermal networks of the semiconductors: Foster and Cauer [40]. The manufacturers are identified four optimal RCs in the datasheet of the semiconductors, and the values of R_i and τ_i have been determined to make the calculations easier.

In this study, a one-cell Cauer thermal model was used to show the thermal behavior of the IGBT and diode. Fig. 2 illustrates this thermal model.

It can be seen that this model can be as a bridge between the power losses and the junction temperature. By employing the state-space equations, these equations will be listed according to the following:

$$x' = \left[-\frac{1}{R_{th}C_{th}}\right]x + \left[\frac{1}{R_{th}C_{th}} \quad \frac{1}{C_{th}}\right]\begin{bmatrix} T_{case} \\ P_{loss} \end{bmatrix} \tag{24}$$

$$\begin{bmatrix} T_{junction} \\ P_{case} \end{bmatrix} = \begin{bmatrix} 1 \\ \left(\frac{1}{R_{th}}\right) \end{bmatrix} x + \begin{bmatrix} 0 & 0 \\ -\frac{1}{R_{th}} & 0 \end{bmatrix}\begin{bmatrix} T_{case} \\ P_{loss} \end{bmatrix} \tag{25}$$

where P_{case} is the heat flow from the junction to the case, P_{loss} is the total semiconductor losses. R_{th} and C_{th} are the junction-to-case thermal resistance and capacitance, respectively.

The values of R_{th} and C_{th} are 0.25 and 0.178 for the IGBT, 0.46 and 0.1023 for the diode, respectively. To complete the thermal model, the heat transfer from the case to the environment through the heatsink should be added. This model is shown in Fig. 3.

In order to implement this part, the thermal elements in the MATLAB environment are used; thus, heat transfer relations must be defined. To provide model, the thermal elements can be attributed to thermal resistance (R) and capacitance (C). The thermal mass is used instead of thermal capacitors, and its energy relationship can be presented as follows [41]:

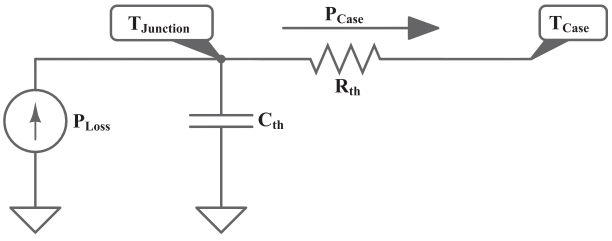

Fig. 2 – The utilized thermal model from junction-to-case.

Please cite this article in press as: Alavi O, et al., Reliability assessment of a stand-alone wind-hydrogen energy conversion system based on thermal analysis, International Journal of Hydrogen Energy (2017), http://dx.doi.org/10.1016/j.ijhydene.2017.04.006

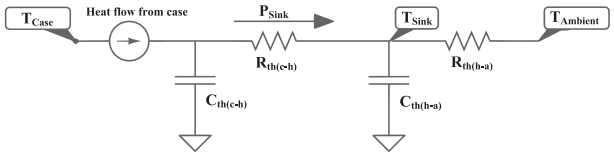

Fig. 3 – The thermal model from case-to-ambient.

$$Q = C_{th}\Delta T = mc_p\Delta T \tag{26}$$

where m is the mass, c_p is the specific heat of the material, and ΔT is the temperature difference. If the specific heat capacity is assumed to be 1, the thermal energy will change as follows:

$$Q = C_{th_{c-h}}\Delta T \tag{27}$$

Thermal energy transfer from the case to the heatsink is as heat conduction between two solid materials. Therefore, the transferred energy will be as follows [42]:

$$Q = \frac{kA\Delta T}{s} \tag{28}$$

where k is the thermal conductivity of the material, A shows the heat transfer area, ΔT is the temperature difference, and s is the thickness. Thermal resistance exhibits the material's ability to resist heat flow, and the opposite is true for the specific thermal resistance [43]. If the values of A and s are equal to 1, the energy relation will be as follows:

$$Q = \frac{\Delta T}{R_{th_{c-h}}} \tag{29}$$

The case-heatsink thermal resistance has been inserted from the module's datasheet, and is equal to 0.05 K/W for the studied module.

Heat transfer between a surface and a moving fluid at different temperatures is known as convection. This convection can occur naturally or by external factors. For thermal energy transfer between the heatsink and the ambient, a convective thermal model is used [44]:

$$Q = hA\Delta T \tag{30}$$

where h is the heat transfer coefficient, A is the surface area, and ΔT is the temperature difference between the material's surface and the ambient. According to the inverse relationship between the heat transfer coefficient and thermal resistance as well as neglecting the surface area [45], the energy will be determined as follows:

$$Q = \frac{\Delta T}{R_{th_{h-a}}} \tag{31}$$

In addition, the implemented MATLAB simulation related to the thermal model from the case to the ambient can be seen in Fig. 4.

In Fig. 4, the block of PS-Simulink (PS S) should be used to turn physical signals to the output MATLAB signal and vice versa. Additionally, attention to the conversion of the temperature from Celsius into Kelvin is absolutely essential. Each physical model connected to the Simscape diagram requires the settings that are provided by f(x) = 0.

As previously mentioned, the heat transfer from the heatsink to the ambient will be made so as to reduce the module temperature and is shown by an external resistor, $R_{th(h\text{-}a)} = 1/\lambda A$. This resistance is quite influenced by the size and type of the cooling system.

In this study, a heatsink – manufactured by Wakefield-Vette – is used, and Fig. 5 depicts the dimensions and the characteristics of the considered heatsink.

For the cooling system, a forced air cooled (500 fpm) heatsink was examined in the analysis. According to [46], the following approximate and simplified relationship can be inferred to calculate the heatsink-ambient thermal resistance for a forced air cooling heatsink:

$$R_{th_{h-a}} = \frac{Performance\ Factor}{Profile\ Perimeter} \tag{32}$$

where the performance factor is determined in terms of the heatsink length and the airflow based on Table 1. The profile perimeter is also the perimeter of the heatsink.

By considering the airflow of 500 fpm and the heatsink length of 10 inches, the heatsink-ambient thermal resistance can be obtained by

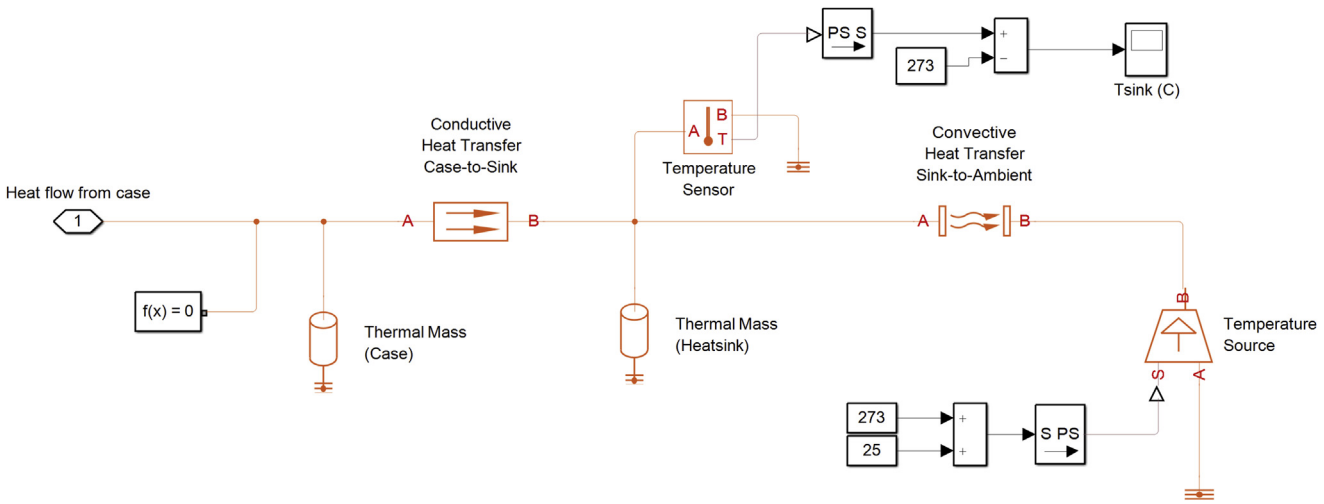

Fig. 4 – The implemented thermal model in MATLAB.

Please cite this article in press as: Alavi O, et al., Reliability assessment of a stand-alone wind-hydrogen energy conversion system based on thermal analysis, International Journal of Hydrogen Energy (2017), http://dx.doi.org/10.1016/j.ijhydene.2017.04.006

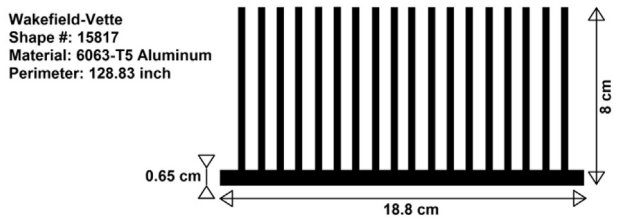

Fig. 5 – The used heatsink in the analysis.

$$R_{th_{h-a}} = \frac{12.95}{128.83} = 0.1005\ ^{\circ}K/W \quad (33)$$

If the value of this resistance is lower, the heatsink performance will be better.

With regard to the electro-thermal modeling, the thermal capacitors prevent the sudden temperature changes under transient conditions, and its variations will be exponential. All module manufacturers only provide the thermal resistance in the datasheet; thus, the capacitor values can be only determined experimentally by measuring the thermal time constant [47]. For simplicity, the case-heatsink thermal capacitance is assumed to be equal to 0.25 J/°K. Also, the heatsink thermal capacitance is selected 0.01 J/°K in accordance to [48].

The overall procedure for reliability assessment of the examined wind-hydrogen system is shown in Fig. 6.

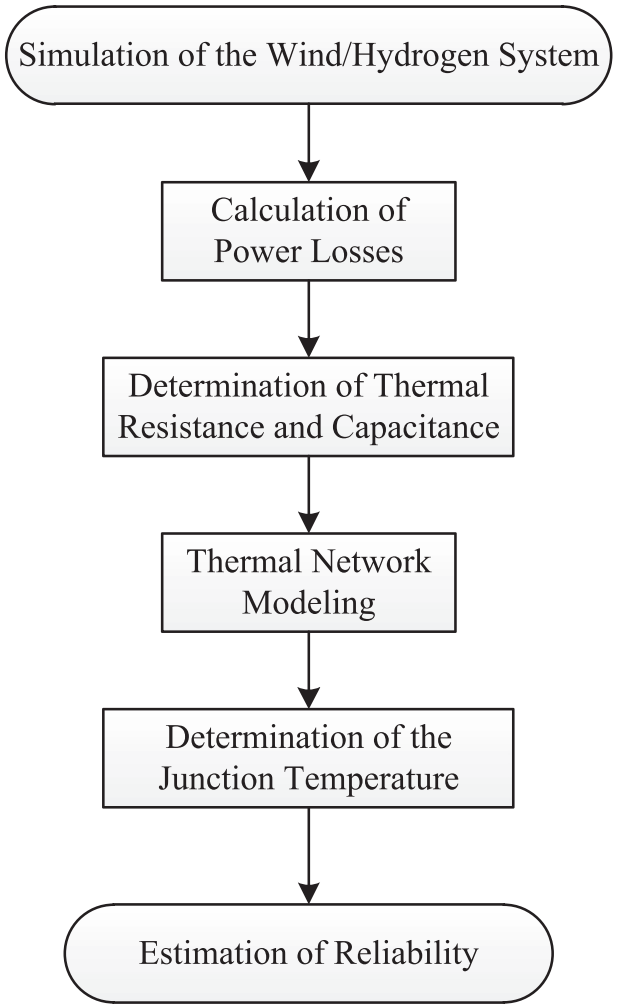

Fig. 6 – The flowchart of reliability assessment of the examined wind-hydrogen system.

Results and discussion

Due to the direct application of power electronic devices in wind-hydrogen systems, estimation of the reliability of the system will significantly reduce the risk of components' failure. This paper reveals a reliability assessment of a nominated wind-hydrogen energy conversion system. According to the importance of the junction temperature in the reliability

Table 1 – . The heatsink performance factor in terms of the airflow and the heatsink length [46].

Heat sink length in inches	Velocity in linear feet per minute (fpm)									
	100	200	300	400	500	600	700	800	900	1000
1.00	91.60	64.77	52.89	45.80	40.96	37.40	34.62	32.39	30.53	28.97
2.00	64.77	45.80	37.40	32.39	28.97	26.44	24.48	22.90	21.59	20.48
3.00	52.89	37.40	30.53	26.44	23.65	21.59	19.99	18.70	17.63	16.72
4.00	45.80	32.39	26.44	22.90	20.48	18.70	17.31	16.19	15.27	14.48
5.00	40.96	28.97	23.65	20.48	18.32	16.72	15.48	14.48	13.65	12.95
6.00	37.40	26.44	21.59	18.70	16.72	15.27	14.13	13.22	12.47	11.83
7.00	34.62	24.48	19.99	17.31	15.48	14.13	13.09	12.24	11.54	10.95
8.00	32.39	22.90	18.70	16.19	14.48	13.22	12.24	11.45	10.80	10.24
9.00	30.53	21.59	17.63	15.27	13.65	12.47	11.54	10.80	10.18	9.66
10.00	28.97	20.48	16.72	14.48	**12.95**	11.83	10.95	10.24	9.66	9.16
11.00	27.62	19.53	15.95	13.81	12.35	11.28	10.44	9.76	9.21	8.73
12.00	26.44	18.70	15.27	13.22	11.83	10.80	9.99	9.35	8.81	8.36
15.00	23.65	16.72	13.65	11.83	10.58	9.66	8.94	8.36	7.88	7.48
16.00	22.90	16.19	13.22	11.45	10.24	9.35	8.66	8.10	7.63	7.24
17.00	22.22	15.71	12.83	11.11	9.94	9.07	8.40	7.85	7.41	7.03
18.00	21.59	15.27	12.47	10.80	9.66	8.81	8.16	7.63	7.20	6.83
20.00	20.48	14.48	11.83	10.24	9.16	8.36	7.74	7.24	6.83	6.48

Please cite this article in press as: Alavi O, et al., Reliability assessment of a stand-alone wind-hydrogen energy conversion system based on thermal analysis, International Journal of Hydrogen Energy (2017), http://dx.doi.org/10.1016/j.ijhydene.2017.04.006

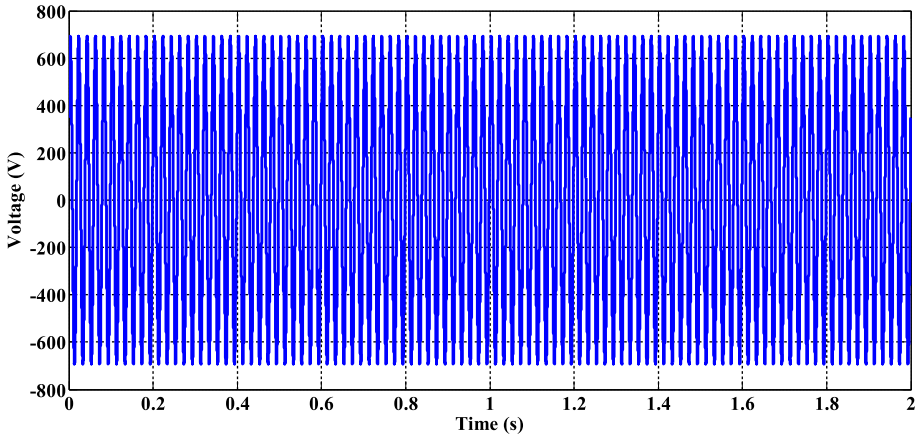

Fig. 7 – The output voltage of the considered wind turbine.

evaluations, an accurate thermal model can provide acceptable results in the analyses. For this reason, the used approach for determining the junction temperature of the switch and the diode was based on a one-cell Cauer model, which exhibits high-speed simulations as well as high precision in the calculations.

The proposed hybrid system was simulated in MATLAB/Simulink. Fig. 7 illustrates the line-to-line output voltage of the wind turbine for phase A.

It is obviously clear that the peak of the wind turbine output voltage is equal to $400\sqrt{3}$. In the rectifier side, the switching state is opposite for upper and lower switches, and they work in 180° towards each other. This means that at any given moment, only one of the switches on each arm is either on or off. This aligns perfectly with the fact that the output voltage of small wind turbines is in the range of 100–400 V (AC or DC) with fixed or variable frequencies [49].

The capacitor between the buck converter and the three-phase rectifier can reflect a DC link, which offers a DC voltage in its two sides. A value of 460 μF was considered for the DC capacitor in the simulation. The output of the rectifier should be a bit smaller than its input. Thus, it can generate almost 600 V, and Fig. 8 demonstrates this consequence. With respect to the duty cycle of the examined buck converter, the fixed output current and voltage of the buck converter can be shown in Fig. 9(a–b). Due to the lack of ideal components in the converter, the voltage and current values have been slightly less than expected.

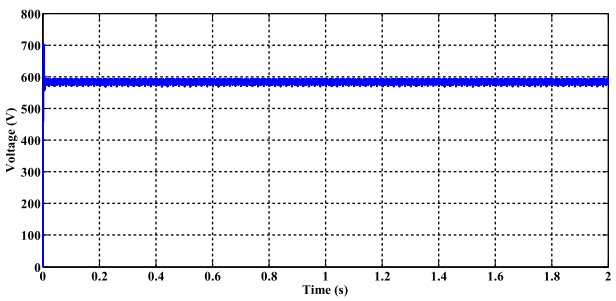

Fig. 8 – The rectifier output voltage.

The used lookup-table method for determining the semiconductors power losses can express the experimental results extracted by the manufacturer. In this analysis, a Fuji 600 V/150 A IGBT module was utilized. Fig. 10 shows the power losses of the diode and the IGBT in the buck converter. The changes of the power losses curves are very similar with the graphs in Ref. [50].

It is obvious that the diode power losses are more than the IGBT, and the diode will handle more stress. Regarding the linear structure of the buck converter, it can be concluded that an increase in the output current leads to a higher junction temperature and also less lifespan.

The diode and IGBT junction temperatures, case temperature, and heatsink temperature can be obtained from the simulation using the considered Cauer model (Fig. 11).

As expected, the junction temperature of the diode is roughly 50% more than the IGBT's junction temperature. All temperatures are fixed at the times above 1.2 s. Additionally, the heatsink is able to cool the case and the module temperatures at the beginning of the operation. However, the used heatsink was not capable to reduce the overall temperature in the future moments of time, and its temperature will be raised to a value of 41 °C. A limitation of 55 °C was also considered for the maximum allowable temperature of the heatsink. The junction temperature curves for the DC–DC converter were validated with regards to [51].

Three legs of the rectifier indicate similar behaviors. Thus, only one of the legs is sufficient for the analysis. The junction temperatures of two IGBTs and two diodes related to phase A are shown in Fig. 12.

As seen, the applied temperature on the diodes is also more than the IGBTs in the rectifier side. In addition, all temperatures in Fig. 12 experience fluctuations, and it happens to the rectifier, but others do not. These fluctuations are due to the sinusoidal pulse-width modulation (similar results are given in Ref. [52]). It also can be concluded that the temperature stress on the rectifier's semiconductors is more than the buck converter, which means the rectifier will require more attention to the maintenance.

As mentioned earlier, a Fuji 600 V/150 A dual-pack IGBT module was used in this study. Therefore, the calculation can

Please cite this article in press as: Alavi O, et al., Reliability assessment of a stand-alone wind-hydrogen energy conversion system based on thermal analysis, International Journal of Hydrogen Energy (2017), http://dx.doi.org/10.1016/j.ijhydene.2017.04.006

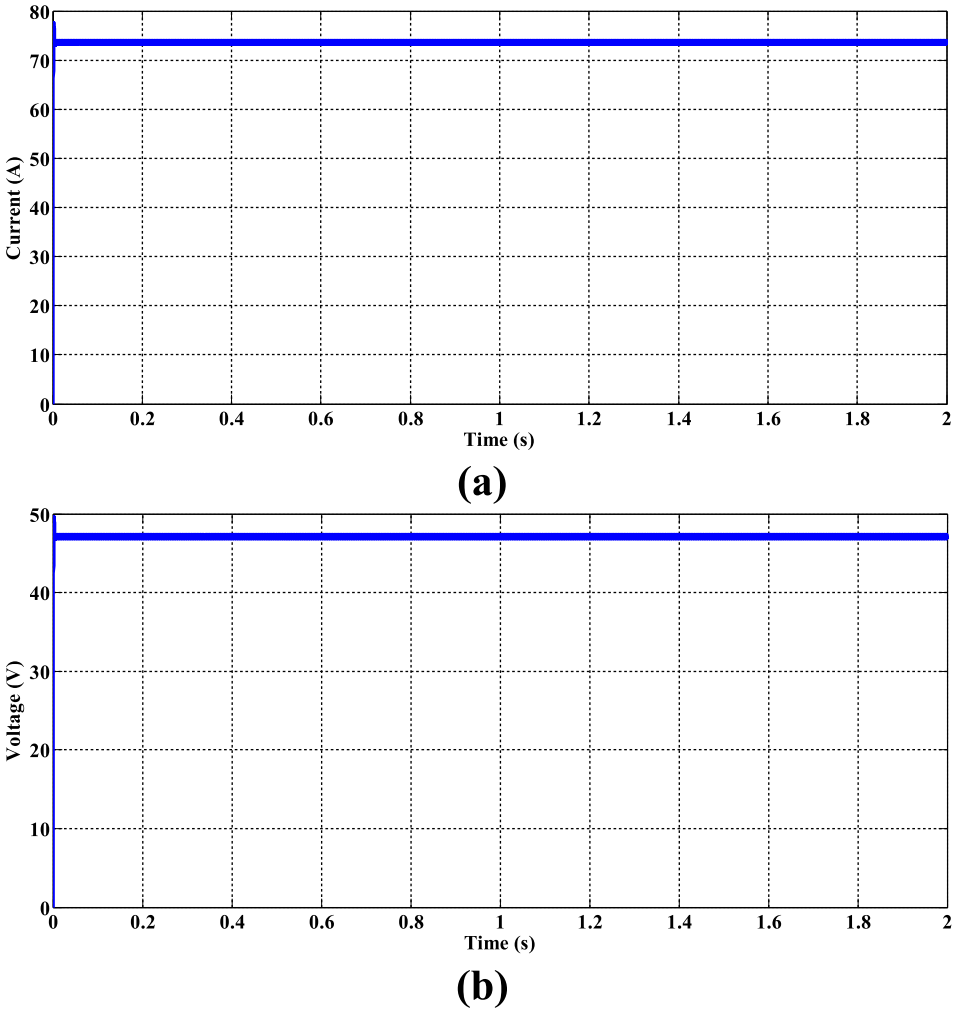

Fig. 9 – The supplied (a) current and (b) voltage of the electrolyzer.

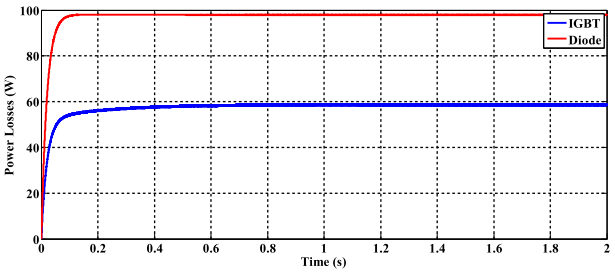

Fig. 10 – The IGBT and diode power losses.

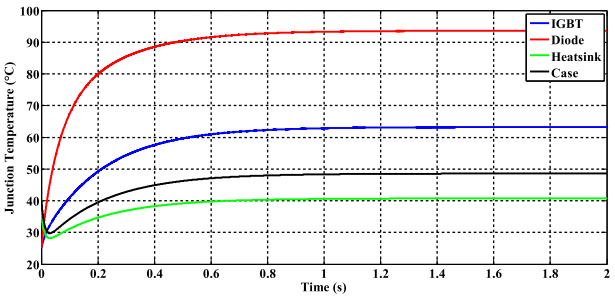

Fig. 11 – The obtained temperatures for the buck converter.

be performed based on this module. Table 2 lists the requirement parameters and their values for predicting the reliability of each component (the quantity for all components is also given).

Assuming the values of 0.8, 25 °C, and 125 °C for the parameters of S, T_A and $T_R(max)$, respectively, the failure rate of the capacitor will depend only on the value of the capacitor.

The total failure rate will be obtained by multiplying the components' failure rates by their quantity, and then the sum

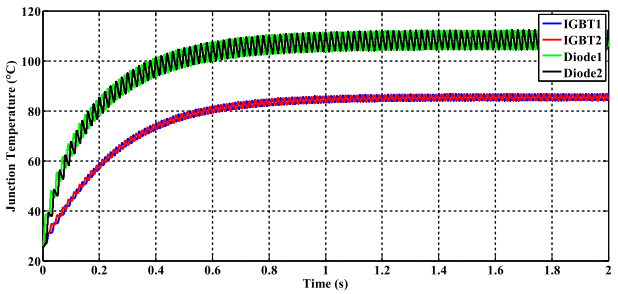

Fig. 12 – The estimated junction temperatures of the IGBTs and diodes in the rectifier side.

Please cite this article in press as: Alavi O, et al., Reliability assessment of a stand-alone wind-hydrogen energy conversion system based on thermal analysis, International Journal of Hydrogen Energy (2017), http://dx.doi.org/10.1016/j.ijhydene.2017.04.006

Table 2 – The predicted failure rate of each circuit's component.

			T_j		Failure rate (failures/10^6 h)	Quantity
IGBTs	Buck DC-DC Converter	IGBT	63.25 °C		1.376	1
	Three-Phase Rectifier	Upper IGBT	85.43 °C		1.961	3
		Lower IGBT	85.43 °C		1.961	3
Diodes			π_S	T_j	Failure rate (failures/10^6 hours)	
	Buck DC-DC Converter	Diode	0.078	93.60 °C	0.075	1
	Three-Phase Rectifier	Upper Diode	0.113	108.34 °C	0.149	3
		Lower Diode	0.113	108.34 °C	0.149	3
Capacitors		Capacitance			Failure rate (failures/10^6 hours)	
	C1	470 μF			0.434	1
	C2	750 μF			0.453	1
Inductor		Inductance			Failure rate (failures/10^6 hours)	
	L	0.45 mH			0.011	1

of all values. Therefore, the failure rate and MTTF for the overall energy conversion system are respectively provided as follows:

$$\begin{aligned}\lambda_{Total} &= 1.376 + (3 \times 1.961) + (3 \times 1.961) + 0.075 + (3 \times 0.149) \\ &\quad + (3 \times 0.149) + 0.434 + 0.453 + 0.011 \\ &= 15.009\, failures/10^6\, hours\end{aligned} \tag{34}$$

$$MTTF_T = \frac{1}{\lambda_{Total}} = 66,629\, hours \tag{35}$$

The calculated MTTF shows that the overall system can operate approximately 7.6 years without any risk and failure. However, the approach mentioned in the MIL-HDBK-217 is conservative with military applications and the system's lifetime may be more than the determined value. Also, it can be found that the rectifier side is under more stresses or failure-prone, and perhaps needs a condition monitoring in order to mitigate the unexpected problems.

Conclusion

In recent years, different renewable resources have been used in order to produce hydrogen as a clean fuel. However, many issues related to hydrogen hybrid systems particularly wind-hydrogen energy conversion systems are not discussed previously. The reliability of a stand-alone wind-hydrogen system was evaluated in this paper, which can be tremendously useful for further studies. The MIL-HDBK-217 was considered, and its relationships were used to calculate the reliability of each system component. Additionally, it was stated that the temperature of semiconductor devices will be the most significant factor in the overall system reliability. Therefore, an accurate thermal network was utilized in order to model the thermal behavior of the semiconductors. Model was simulated by the MATLAB software. The outcomes illustrated that the diode junction temperature is approximately 50% more than the IGBT in the buck converter. Also, the results showed that the thermal stresses of the rectifier components are higher than those of the buck converter. This means that the possibility of failure in the rectifier is much higher than the buck DC–DC converter. Nonetheless, the MTTF of the wind-hydrogen system was conservatively estimated to be 7.6 years.

The issue of reliability is very important to the manufacturers, because it will have positive effects on competition on the market. Thus, an accurate estimation for the power electronic devices' lifetime (as the most failure-prone component) can provide the possibility to compare the different types of energy conversion systems, particularly hydrogen energy. Additionally, the reliability assessment and comparison of different topologies for power electronic circuits (e.g., synchronous buck converters) can be made as future work.

REFERENCES

[1] Huang PH, Kuo JK, Wu ZD. Applying small wind turbines and a photovoltaic system to facilitate electrolysis hydrogen production. Int J Hydrogen Energy 2016;41(20):8514–24.
[2] Luna-Rubio R, Trejo-Perea M, Vargas-Vazquez D, Rios-Moreno GJ. Optimal sizing of renewable hybrids energy systems: a review of methodologies. Sol Energy 2012;86:1077–88.
[3] Siyal SH, Mentis D, Howells M. Economic analysis of standalone wind-powered hydrogen refueling stations for road transport at selected sites in Sweden. Int J Hydrogen Energy 2015;40:9855–65.
[4] Samsatli S, Staffell I, Samsatli NJ. Optimal design and operation of integrated wind-hydrogen-electricity networks for decarbonising the domestic transport sector in Great Britain. Int J Hydrogen Energy 2016;41:447–75.
[5] Mostafaeipour A, Khayyami M, Sedaghat A, Mohammadi K, Shamshirband S, Sehati M-A, et al. Evaluating the wind energy potential for hydrogen production: a case study. Int J Hydrogen Energy 2016;41:6200–10.
[6] Olateju B, Kumar A, Secanell M. A techno-economic assessment of large scale wind-hydrogen production with energy storage in Western Canada. Int J Hydrogen Energy 2016;41:8755–76.
[7] Hacatoglu K, Dincer I, Rosen MA. Sustainability of a wind-hydrogen energy system: assessment using a novel index and comparison to a conventional gas-fired system. Int J Hydrogen Energy 2016;41:8376–85.

Please cite this article in press as: Alavi O, et al., Reliability assessment of a stand-alone wind-hydrogen energy conversion system based on thermal analysis, International Journal of Hydrogen Energy (2017), http://dx.doi.org/10.1016/j.ijhydene.2017.04.006

[8] Ghandehariun S, Kumar A. Life cycle assessment of wind-based hydrogen production in Western Canada. Int J Hydrogen Energy 2016;41:9696–704.
[9] Weidong G, Zhuoyong Y. Research on non-grid-connected wind power/water-electrolytic hydrogen production system. Int J Hydrogen Energy 2012;37:737–40.
[10] Chade D, Miklis T, Dvorak D. Feasibility study of wind-to-hydrogen system for Arctic remote locations – Grimsey island case study. Renew Energy 2015;76:204–11.
[11] Aiche-Hamane L, Belhamel M, Benyoucef B, Hamane M. Feasibility study of hydrogen production from wind power in the region of Ghardaia. Int J Hydrogen Energy 2009;34:4947–52.
[12] Greiner CJ, KorpÅsb M, Holen ATA. Norwegian case study on the production of hydrogen from wind power. Int J Hydrogen Energy 2007;32:1500–7.
[13] Rama P, Chen R, Andrews J. A review of performance degradation and review models of hydrogen fuelled polymer electrolyte fuel cells. J Power Energy 2008;222:421–41.
[14] Whiteley M, Fly A, Leigh J, Dunnett S, Jackson L. Advanced reliability analysis of Polymer Electrolyte Membrane Fuel Cells using Petri-Net analysis and fuel cell modelling techniques. Int J Hydrogen Energy 2015;40:11550–8.
[15] Phan DT, Chung GS. Reliability of hydrogen sensing based on bimetallic NiePd/graphene composites. Int J Hydrogen Energy 2014;39:20294–304.
[16] Boon-Bretta L, Bousek J, Moretto P. Reliability of commercially available hydrogen sensors for detection of hydrogen at critical concentrations: part II – selected sensor test results. Int J Hydrogen Energy 2009;34:562–71.
[17] Boon-Brett L, Bousek J, Castello P, Salyk O, Harskamp F, Aldea L, et al. Reliability of commercially available hydrogen sensors for detection of hydrogen at critical concentrations: Part I – testing facility and methodologies. Int J Hydrogen Energy 2008;33:7648–57.
[18] Agbossou K, Lal Kolhe M, Hamelin J, Bernier E, Bose TK. Electrolytic hydrogen based renewable energy system with oxygen recovery and re-utilization. Renew Energy 2004;29:1305–18.
[19] Hahn B, Durstewitz M, Rohrig K. Reliability of wind turbines. In: Wind energy. Springer B; 2007. p. 329–32.
[20] Pérez JMP, Márquez FPG, Tobias A, Papaelias M. Wind turbine reliability analysis. Renew Sustain Energy Rev 2013;23:463–72.
[21] http://www.srcgreenpower.com/wind200/[Accessed 16 March 2017].
[22] Erikson RW. Fundamentals of power electronics. 1997. New York.
[23] MIL-HDBK-217F (Notice 2). Military handbook: reliability prediction of electronic equipment. 1995.
[24] FIDES reliability methodology for electronic systems. 2009. Available, www.fides-reliability.org.
[25] He J, Morris WL, Shaw MC, Mather JC, Sridhar N. Reliability in large area solder joint assemblies and effects of thermal expansion mismatch and die size. Int J Microcircuits Electron Packag 1998;21(3):297–305.
[26] Alavi O, Hooshmand-Viki A, Shamlou S. A comparative reliability study of three fundamental multilevel inverters using two different approaches. Electronics 2016;5(2):1–18.
[27] Song Y, Wang B. Survey on reliability of power electronic systems. IEEE Trans Power Electron 2013;28(1):591–604.
[28] Wang H, Ma K, Blaabjerg F. Design for reliability of power electronic systems. In: IEEE industrial electronics society annual conference (IECON). Canada: Montreal; Oct 2012. p. 25–8.
[29] Birolini A. Reliability engineering. Berlin: Springer; 2004.
[30] Rausand M, Hoyland A. System reliability theory: models, statistical methods, and applications. Wiley; 2004.
[31] Zini G, Mangeant C, Merten J. Reliability of large-scale grid-connected photovoltaic systems. Renew Energy 2011;36:2334–40.
[32] RCA release TR-1100. Reliability stress analysis for electronic equipment. US Dept of Commerce; 1956.
[33] Abdi B, Ranjbar AH, Gharehpetian GB, Milimonfared J. Reliability considerations for parallel performance of semiconductor switches in high-power switching power supplies. IEEE Trans Ind Electron 2009;56:2133–9.
[34] Blake C, Bull C. IGBT or MOSFET: choose wisely. International Rectifier.
[35] Wheeler P, Clare J, Lillo LD, Bradley K, Aten M, Whitley C, et al. A reliability comparison of a matrix converter and an 18-pulse rectifier for aerospace applications. In: 12th international power electronics and motion control conference, portoroz, Slovenia; 30 Aug 2006.
[36] Walters K. Rectifier reverse switching performance. Microsemi, MicroNote Ser 1998;302.
[37] IGBT power losses calculation using the data-sheet parameters. Infineon; 2010.
[38] Yang K. Transient electro-thermal analysis of traction inverters. Master Thesis. McMaster University; 2014.
[39] Ammous A, Ghedira S, Allard B, Morel H, Renault D. Choosing a thermal model for electrothermal simulation of power semiconductor devices. IEEE Trans Power Electron 1999;14(2):300–7.
[40] Firouz Y, Bina MT, Eskandari B. Efficiency of three-level neutral-point clamped converters: analysis and experimental validation of power losses, thermal modelling and lifetime prediction. IET Power Electron 2014;7(1):209–19.
[41] https://en.wikipedia.org/wiki/Thermal_mass [Accessed 16 March 2017].
[42] http://www.engineeringtoolbox.com/conductive-heat-transfer-d_428.html [Accessed 16 March 2017].
[43] http://www.engineeringtoolbox.com/thermal-resistivity-d_1053.html [Accessed 16 March 2017].
[44] http://www.engineeringtoolbox.com/convective-heat-transfer-d_430.html [Accessed 16 March 2017].
[45] https://neutrium.net/heat_transfer/thermal-resistance/ [Accessed 16 March 2017].
[46] Simplified method for estimating heat sink thermal resistance, semikron. 2014.
[47] Staric P, Margan E. Wideband amplifiers. Dordrecht: Springer; 2006.
[48] Schonberger J. Thermal simulation of a buck converter. Plexim GmbH. 2010.
[49] Staffell I, Brett DJL, Brandon NP, Hawkes AD. Domestic microgeneration: renewable and distributed energy technologies, policies and economics. London: Routledge; 2015.
[50] Lkonen M. Power cycling lifetime estimation of IGBT power modules based on chip temperature modeling. PhD Thesis. Lappeenranta University of Technology; 2012.
[51] Ahmed MMR, Putrus GA. A method for predicting IGBT junction temperature under transient condition. In: 34th annual conf ind electron; 2008. p. 454–9. http://dx.doi.org/10.1109/TIA.2015.2391438.
[52] Ma K, Bahman AS, Beczkowski S, Blaabjerg F. Complete loss and thermal model of power semiconductors including device rating information. IEEE Trans Power Electron 2015;30(5):2556–69.

Please cite this article in press as: Alavi O, et al., Reliability assessment of a stand-alone wind-hydrogen energy conversion system based on thermal analysis, International Journal of Hydrogen Energy (2017), http://dx.doi.org/10.1016/j.ijhydene.2017.04.006